A NOVEL METHOD FOR PASSIVE DIGITAL IMAGE ACQUISITION FROM A SCANNING ELECTRON MICROSCOPE

By

C2009
Joseph Sylvester Makarewicz

Submitted to the Department of Electrical Engineering and Computer Science
and the Faculty of the Graduate School of the University of Kansas
in partial fulfillment of the requirements for the degree of
Master of Science

____
Dr. Arvin Agah (Committee Chair)

____
Dr. Carl Leuschen (Committee Member)

____
Dr. Brian Potetz (Committee Member)

____
Date Defended

Joseph Sylvester Makarewicz
The Thesis Committee for Joseph Sylvester Makarewicz certifies
that this is the approved version of the following thesis:

A NOVEL METHOD FOR PASSIVE DIGITAL IMAGE ACQUISITION
FROM A SCANNING ELECTRON MICROSCOPE

Committee:

____
Committee Chair

____
Committee Member

____
Committee Member

____
Date Defended

ABSTRACT

The Center for Nanotechnology at NASA Ames Research Center is developing a micro-column scanning electron microscope with energy-dispersive x-ray spectroscopy (MSEMS). The MSEMS has the potential for space explorations because it is lightweight, low power and has superior analytical capabilities, including imaging with sub-micrometer resolution and elemental analysis. The image acquisition software for the MSEMS is currently in its early stages of development. The development of the image acquisition software has lead to the research problem addressed in this thesis.

The objective of this thesis is to provide a detailed explanation of a novel algorithm for obtaining digital images from a scanning electron microscope (SEM). An introduction to the SEM is presented including its theory of operation and current research. Established methods for digital image acquisition from an SEM are summarized, all of which exploit electron beam position. A new method for digital image acquisition is introduced, which disregards electron beam position. The hardware requirements for the new method are discussed. The model for the new method is fully developed. Manual and automated methods for determining the model parameters are explained. Some preliminary results are shown. Some advantages and disadvantages of the method are discussed and the future work is recommended.

ACKNOWLEDGEMENTS

I would like to thank all my advisors and colleagues that have supported and directed me through this research. Dr. Arvin Agah was my faculty advisor and my committee chair on my thesis committee. Dr. Carl Leuschen and Dr. Brian Potetz were two of my professors during my graduate work and served on my thesis committee. Cattien V. Nguyen proposed this research problem and was also my NASA advisor during this research. Bryan Ribaya is a doctoral student at Santa Clara University and is primarily responsible for the research and development the MSEMS. Darrell Niemann is a post doctoral researcher at NASA that has been contributing to the development of the MSEMS through the electronic characterization and modeling of carbon nanotubes.

I would especially like to thank my wife, Heather, for her support, guidance, and patience throughout my hectic graduate and undergraduate studies. She has been a stabilizing influence in my life. She has reminded me that there is more to life than studying and research. She has helped me to keep boundaries between my work and my personal life. Together, we are discovering recreational activities which we both enjoy. She has brought me enjoyment and fulfillment that cannot be discovered in research and study.

This material is based upon research that was funded in part by Education Associates at NASA Ames Research Center. Any opinions, findings, and conclusions or recommendations expressed in this material are those of the authors and do not necessarily reflect the views of the National Aeronautics and Space Administration.

CONTENTS

ABSTRACT iii

ACKNOWLEDGEMENTS iv

CONTENTS v

1. Introduction 1
2. SEM Imaging Process 1
3. Current SEM Research in Nanotechnology 6
4. Related Work 7
   - 4.1 Frame Grabbing 8
   - 4.2 Analog to Digital Converter Sampling 9
   - 4.3 Digitally-Controlled Electron Beam Position 11
5. Methods 12
   - 5.1 Hardware Requirements 12
   - 5.2 Model Assumptions 13
   - 5.3 Model Description 14
   - 5.4 Model Parameters 15
   - 5.5 Number of Samples per Row (N_{spr}) 16
   - 5.6 Number of Rows (N_r) 19
   - 5.7 Number of Samples between Rows (N_{sbr}) 21
   - 5.8 Number of Initial Samples (N_{is}) 22
6. Results 24
7. Limitations 26
8. Discussion 27

9. Future Work ... 29

10. Further Applications ... 30

11. Conclusion ... 31

REFERENCES ... 32

1. Introduction

The scanning electron microscope (SEM) is a scientific research instrument that is frequently used in both the natural and applied sciences. The SEM is popular due to its ability to produce high resolution images and determine elemental composition. When compared to the optical microscope, the SEM has superior imaging capabilities. The optical microscope has a maximum resolution of around 200nm, a maximum magnification of around 1,000x, and a narrow depth of field. Where as, the SEM currently has a nominal resolution less than 10nm, a maximum magnification of around 10,000x, and a large depth of field. The SEM has superior imaging capabilities because it uses electrons, instead of photons, to create an image. During the SEM imaging process, characteristic x-rays are emitted from the surface of the sample. The characteristic x-rays allow the SEM to determine elemental composition through x-ray spectroscopy [1].

2. SEM Imaging Process

Inside a vacuum chamber, an SEM produces an image through the following process. The electron gun generates an electron beam. The focusing coils, or lenses, focus the electron beam onto a small spot on the sample. When the electron beam strikes the sample, characteristic x-rays emit from the sample as some of the electrons are absorbed and others are scattered. Specialized sensors, called electron detectors, detect the different types of electrons. An image is formed by sampling the electron detectors while scanning the electron beam over the surface of the sample. The electron beam is scanned in a raster pattern with the scanning coils [1]. Figure 1 illustrates the main components of an SEM column.

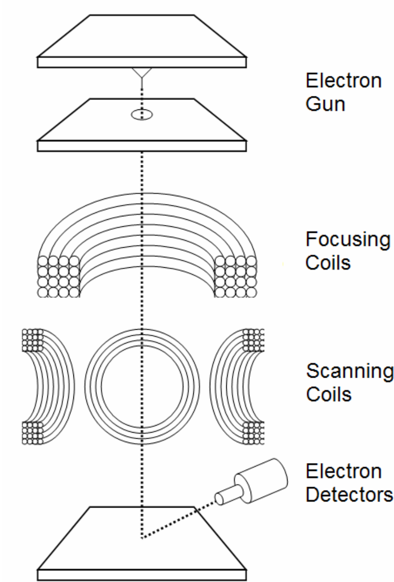

Figure 1: SEM Column

The SEM imaging process occurs in a vacuum chamber. Most SEMs operate in high vacuum, but the environmental SEM (ESEM) can operate in low vacuum [1]. A vacuum pump or an ion pump can be used to achieve a vacuum chamber. A vacuum pump physically suctions the particles from the chamber. An ion pump charges the particles within the chamber and attracts them using a high electric field [2]. During SEM operation, an ion pump cannot be use to maintain the vacuum chamber because of its high electric field. As a vacuum electronic, the SEM is well-suited for space applications. A vacuumed chamber can be simply achieved by opening the chamber to the vacuum of space. A properly vacuumed chamber is important for the SEM. The vacuum chamber is free of particles that will obstruct the path of the electrons. Any particles remaining in the chamber may become ionized by the electrons generated from the electron gun [1].

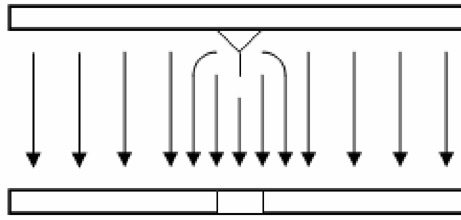

Figure 2: Electric Fields of a Cold Field Emission Electron Gun

Within the SEM, the electron gun generates the electron beam [1]. Electron beams are currently generated in one of two methods. An inefficient method for electron beam generation is thermionic emission. In thermionic emission, electrons are emitted by passing electronic current through a heating element, which is usually made from tungsten. A significantly more efficient method for electron beam generation is cold field emission. With cold field emission, an electric field is applied between a cathode and an anode. The cathode has a sharp point that is aligned with a small hole in the anode. The electric field is enhanced at the sharp point on the cathode. Figure 2 shows the electric fields of a cold field emission electron gun. The electric field extracts electrons from the sharp point and accelerates them towards the anode. Some of the electrons are absorbed by the anode. Others electrons pass through the small hole in the anode and form an electron beam. This process is similar to electrons leaking across the plates in a parallel plate capacitor. The electron gun can be applied to many applications. Using the electron beam from the electron gun, ion beams, light, and x-rays can be created [3]. In the SEM, a narrow beam must be produced by the electron gun. With a narrower electron beam, the SEM will be able to achieve a higher spatial resolution [1].

The electron beam generated by an electron gun may not be narrow. The electrons may disperse after passing through the narrow hole of the extracting anode. Focusing coils,

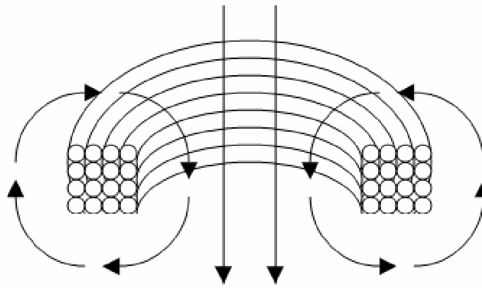

Figure 3: Electric Fields of a Coiled Inductor

which are also called lenses, are used to narrow the electron beam. The focusing coils are large open core inductors whose electric fields squeeze the electron beam. With the focusing coils, the electron beam is perpendicular to the coils and it passes through the center of the coils. The field created by the coils is in the direction of the electron beam. Figure 3 shows the electric fields for an open core coiled inductor. The focus of the electron beam can be varied by varying the current through the focusing coils. Once the beam is focused, the electron beam is positioned on the sample using the scanning coils. The scanning coils are large inductors that bend the electron beam. With the scanning coils, the electron beam is parallel to the coils and the electron beam does not pass through the center of the coils. The scanning coils create electric fields that are perpendicular to the electron beam. The perpendicular forces cause the beam to bend and change the position of the electron beam. The position of the electron beam can be varied by varying the current through the inductors. There are four scanning coils that work together in pairs. One pair adjusts the x-position and the other pair adjusts the y-position. By controlling the current through the scanning coils, the electron beam is scanned over the surface of the sample in a raster pattern [1].

Special sample preparation is required before a sample can be imaged by an SEM. Samples should be cleaned of loose particles before entering the SEM to prevent contamination of the SEM. Samples cannot give off particles while under a vacuum. Samples should be conductive so that a static charge does not build up during the imaging process. Non-conductive samples are usually coated with a thin layer of conductive material. A thin layer of conductive material can be created using ion beam sputtering or chemical vapor deposition. An ion beam sputter shoots a beam of ions at a target containing the material being deposited. The ions collide with the target and remove some of the material which is then deposited on the sample. Chemical vapor deposition vaporizes the conductive material and deposits it on the surface of the sample [1].

When the electron beam strikes the sample, some of the electrons are absorbed and others are scattered. The electrons that are scattered are called back scattered electrons (BSE). BSE have high kinetic energy. BSE are detected to show differences in chemical composition. The electrons that are not back scattered are absorbed by the sample. Some of the absorbed electrons displace other electrons from the sample. The electrons emitted from the sample are called secondary electrons (SE). SE have low kinetic energy. SE are detected to show differences in topography. Specialized sensors, called electron detectors, are used to detect electrons. Separate electron detectors collect the different types of electrons. Since SE have low kinetic energy, they must be attracted to the electron detector using a weak electronic field. The electron detector collects the electrons creating an electric current. The electric current is amplified for ease of measurement.

The Everhart-Thornley detector is one of the oldest and most commonly used detectors. It uses a photo multiplier to amplify the current [1].

3. Current SEM Research in Nanotechnology

The basic principles of the SEM were developed in the late 1930s and early 1940s. Since then, the SEM has been incrementally improved through research and development [4]. The Center for Nanotechnology at NASA Ames Research Center intends to continue to improve the SEM using nanotechnology.

An area of current research is the development of an efficient, mechanically robust electron gun which produces a narrow electron beam. Electron gun technology may be improved by incorporating carbon nanotubes. Due to their strong chemical bonds, carbon nanotubes are mechanically strong and are expected to degrade slowly over time [5, 6]. Both bundles of carbon nanotubes and individual carbon nanotubes have been investigated [6-16]. Using photolithography, patterning processes have been developed for growing arrays of bundles of carbon nanotubes. Bundles of carbon nanotubes have potential use in high current applications. They can create electron beams with a higher charge density, but create wider electron beams [7-9]. On the other hand, individual carbon nanotubes can create narrow electron beams, but cannot provide a high charge density [10-14]. Individual carbon nanotubes can create a narrow beam because they have a very small diameter and are nearly atomically sharp [5]. A narrow electron beam may be obtained by incorporating an individual carbon nanotube into a cold field emitter.

If an electron gun can produce a narrow electron beam, then fewer focusing coils are required in the SEM. The focusing coils are large open core inductors whose electric fields narrow the electron beam. Another recent technology has made it possible to remove the scanning coils from the SEM. The scanning coils are large inductors whose electric fields set the electron beam position by bending it. A nano-positioning stage can replace the scanning coils. Nano-positioning stages use linear peizo motors with capacitive feedback to achieve high resolutions that are currently about 1nm. The nano-positioning stage can change the electron beam position by physically moving the electron gun [14].

After improving the SEM with nanotechnology, it is expected to have less than 10nm resolution. By removing the focusing and scanning coils, the size and weight of the SEM will be significantly reduced. Using nanotechnology, the SEM will be improved and will be more ideal for space applications [14].

4. Related Work

Modern SEMs are digitally controlled and produce high resolution digital images. Where as, older SEMs have analog control and a cathode ray tube monitor. In the past, digital images were acquired from analog SEMs by photographing the cathode ray tube monitor. Several modern solutions have been proposed for acquiring a digital image from an analog SEM. This thesis proposes a novel solution to this problem.

4.1 Frame Grabbing

A digital SEM image can be acquired using a frame grabbing device. The frame grabbing device can digitize the video signal going to the cathode ray tube monitor. Over the past 20 years, several methods have proposed to use a frame grabbing device for SEM digital image acquisition [17-20].

In 2006, Knapp et al. developed a flexible system for SEM control and digital image acquisition. A personal computer controls 6 high voltage power supplies and 8 current supplies. The personal computer is equipped with a frame grabber for acquiring the digital SEM image. The system required a significant amount of hardware and software development. The system was adaptable for use with 3 different SEMs [17, 18].

In 1996, Postek and Vladar developed a similar system for SEM control and digital image acquisition named Isaac. The system was based on a personal computer with an SEM control card and a frame grabber. The SEM control card has digital to analog converters (DAC) that send control signals to the SEM power supplies. It also has analog to digital converters (ADC) for measuring data from electron detectors. The frame grabber captured digital images from the SEM monitor. The system was able to capture high resolution images. The system was only applied to a single SEM. It was unique because could not only acquire image, but is could also perform image processing [19].

In 1994, Ang et al. proposed using a commercially available frame grabber to acquire digital images from an analog SEM. The frame grabber replaced the typical Polaroid

photograph system. Few modifications were made to the SEM. The method required locating and connecting into the video signal and the synchronization signal going to the SEM monitor. The digital SEM image acquisition system was only applied to a single SEM, but could be applied to any SEM [20].

In the method proposed in this thesis, a frame grabbing device is not employed. However, the proposed method is similar to a frame grabber. In fact, the proposed method can be used in place of a frame grabber. Frame grabbers obtain images from video signals which include horizontal and vertical synchronization signals. The proposed system can obtain an image from a video signal without using the horizontal and vertical synchronization signals.

4.2 Analog to Digital Converter Sampling

A digital image can also be acquired by sampling the electron detector with an analog to digital converter that is synchronized with position of the electron beam. Over the past 20 years, several methods have proposed to use an analog to digital converter for SEM digital image acquisition [21-24].

In 2006, Russev et al. developed a system that could be used for electron beam lithography as well as SEM control and digital image acquisition. The system is a low cost, microcontroller based device that is connected to a personal computer. The microcontroller has DACs that send control signals to the SEM power supplies and ADCs for measuring data from electron detectors. The system required an extensive

amount of hardware and software development. The system was built for a single SEM, but has some built-in flexibility for being adapted to other SEM [21].

In 1998, Gebert and Preiss proposed a method using a commercially available ADC to acquire digital images from an SEM. A laboratory containing an SEM will likely contain a computer for data acquisition that has an ADC. For the method, the ADC is triggered using the line blank signal from the SEM. Few modifications were made to the SEM. The most difficult part of the method is locating and connecting into the video signal and the synchronization signal. Software must be written to configure and acquire data from the ADC. The digital SEM image acquisition system was only applied to a single SEM, but could be applied to any SEM [22].

In 1998, Edgerton and Wan developed a method for SEM control and digital image acquisition using a data acquisition card. The method allows the SEM to operate normally when not acquiring a digital image. When acquiring a digital image, the DACs send control signals to the SEM scan amplifiers and the ADCs measure data from electron detectors. Software was written using the drivers from the data acquisition card. This method was applied to a single SEM and would require modifications for other SEMs or data acquisition cards [23].

In 1992, Dubson and Zhu developed a passive method for SEM digital image acquisition using an ADC. The ADC connected to the video, horizontal and vertical synchronization signal connect to the SEM CRT monitor. The ADC had a fixed sampling rate of 20 kHz,

which limited the method to a single scan speed. Specialized software and hardware were developed for the method. The method would have to be modified for other SEM [24].

In the proposed method, a digital image will be formed by sampling the electron detector with an analog to digital converter. Unlike previous approaches, the proposed method is not synchronized with the electron beam position. The proposed method infers the electron beam position from the samples collected from the electron detector.

4.3 Digitally-Controlled Electron Beam Position

In addition to obtaining a digital image, some solutions also choose to digitally control the electron beam position [17-19, 21, 23]. Knapp et al purchased modern high voltage power supplies that could be digitally controlled using a PC [17, 18]. Postek et al. and Edgerton et al. used a computer and a DAC to control the existing SEM scanning power supplies [19,23]. Russev et al. used a microcontroller containing a DAC to control the existing SEM scanning power supplies [21]. All of these systems actively control the imaging process. Therefore, they can achieve high resolution images but have increased hardware and software complexity.

In the proposed method, hardware is not developed to control the electron beam position. Rather, the electron beam position is controlled by the existing analog SEM. The proposed method can passively acquire a digital image without affecting the normal SEM functionality.

5. Methods

Following a raster pattern, the SEM scans the electron beam over the surface of the sample. The SEM is controlling the electron beam position and measuring the electron detector. It easily forms an image by associating the measurements from the electron detector with the electron beam position. The SEM easily forms an image due to its knowledge of the electron beam position. As described in related work, several methods have been proposed for obtaining a digital image from an SEM. This thesis presents the hardware requirements for obtaining a digital image from an SEM without knowledge of the electron beam position. An algorithm for forming the SEM image from a set of discrete samples is also presented.

5.1 Hardware Requirements

The SEM creates an image by scanning the electron beam over the sample in a raster pattern while measuring the current from the electron detector. The electron detector is a specialized sensor that collects and amplifies electrons. The electron detector can be simply modeled as a variable current source that is dependent on the number electrons it collects. The internal resistance of the SEM converts the current from the electron detector into a small voltage. In the proposed method, this small voltage is measured.

The hardware requirements for this method are minimal. This method requires a high speed, high impedance analog to digital converter to measure the small voltage. As shown in Figure 4, the hardware for this method is an SEM with a single analog to digital converter (ADC) and a personal computer (PC). The personal computer uses the

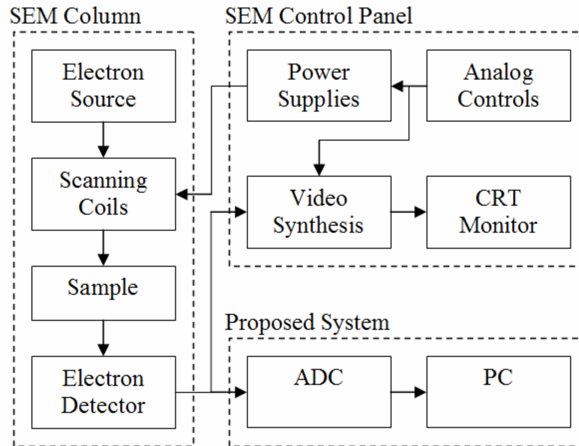

Figure 4: Proposed System for Digital Image Acquisition from an SEM

algorithm presented in this paper to form an image. This method is unique because it only measures the electron detector signal going from the SEM Column to the SEM Control Panel.

5.2 Model Assumptions

This method does not directly monitor the position of the electron beam. However, the raster pattern of the electron beam must be known. Most SEMs control the electron beam in a zigzag raster pattern similar to Figure 5. The beam moves slowly when it moves horizontally, as indicated by the back arrows, and fast when it moves diagonally, as indicated by the gray arrows. This method assumes a zigzag raster pattern.

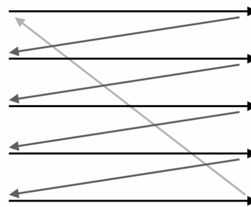

Figure 5: SEM zigzag raster pattern

The horizontal scan rate of the electron beam is selected by the user. The sampling rate of the ADC must vary depending on the horizontal scan rate of the electron beam. If the electron beam is scanning slowly, then the ADC must sample slowly. Likewise, if the electron beam is scanning faster, then the ADC must sample faster. A precise relationship exists between the horizontal scanning rate and the sampling rate of the ADC. This model assumes that the ADC is acquiring numerous samples per horizontal scan, so that there are numerous samples per row in the final image.

Since the location of the electron beam is not known, the sampling may start anywhere along the raster pattern. If the ADC samples over the time for two complete raster scans, then there is guaranteed to be at least one continuous, complete raster scan. This model assumes that samples are collected for at least two complete raster scans.

5.3 Model Description

The digitized measurements from the electron detector form a set of discrete samples that must be manipulated to create a digital image. Since the location of the electron beam is not known, the sampling may start anywhere along the scanning raster pattern. If the ADC samples over the time for two complete raster scans, then there must be one continuous, complete raster scan. In other words, in the set of samples, there are some initial samples that belong to the previous scan and there are some final samples that belong to the next scan. The number of initial samples to discard is one parameter that must be determined. The data used to construct the image is obtained during the horizontal scans, indicated by the black arrows in Figure 5.

During the horizontal scan of each row, approximately the same numbers of samples are obtained. The average number of samples per row, or samples per horizontal scan, is another parameter that must be determined. Unnecessary data is obtained during the diagonal scans, indicated by the gray arrows in Figure 5. During the diagonal scans, an average number of samples are acquired. The average number of samples per diagonal scan, or the average number of samples in between rows, is another parameter the must be determined. During each complete raster scan, fixed number of rows is scanned. The number of rows is final parameter that must be determined.

5.4 Model Parameters

Therefore, in order to create a digital image from the set of samples, there are four parameters of the series of samples that must be optimized: the number of initial samples to remove (N_{is}), the number of samples per row (N_{spr}), the number of samples between rows to remove (N_{sbr}), and the number of rows (N_r). Figure 6 illustrates the parameters of the series of samples that must be optimized in order to form an image.

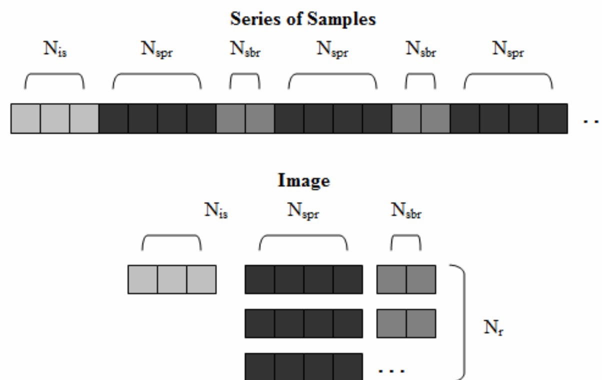

Figure 6: Optimization Parameters

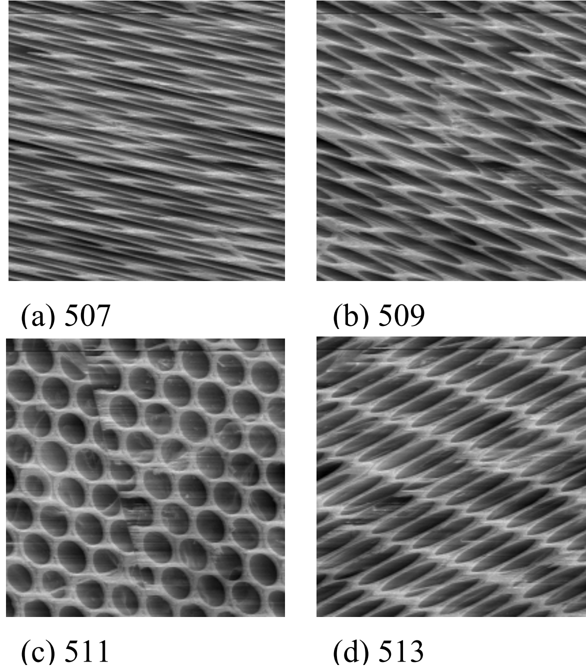

Figure 7: Varying Number of Samples per Row (N_{spr})
$N_r = 512$, $N_{sbr} = 0$, $N_{is} = 0$

5.5 Number of Samples per Row (N_{spr})

The number of samples per row sets the width of the final image. The number of samples per row is the most critical parameter to determine. Figure 7 shows how varying the number of samples per row affects the image. The image with the optimum number of samples per row is in Figure 7c.

If the horizontal scanning rate of SEM and the sampling frequency of the analog to digital converter are known, then the number of samples per row can be calculated using Equation 1.

$$N_{spr} = \frac{F_s}{F_{sc}} \tag{1}$$

In Equation 1, N_{spr} is the number of samples per row, F_s is the sampling frequency in samples per second, and F_{sc} is the scanning rate of the SEM in lines per second, or rows per second. The scanning rate of the SEM can be approximated by estimating how long the SEM takes to refresh one line of the image on the cathode ray tube.

The number of samples per row can also be inferred from the series of samples. An SEM image is an example of a natural image. In natural images, low spatial frequencies are more predominant than high spatial frequencies. As a result, neighboring pixels have similar intensities. Therefore, the surface formed by image intensities is relatively smooth except at object edges. When the image has the correct number of samples per row, then the image will be horizontally and vertically smooth.

A simple method for evaluating the smoothness of an image is to sum the finite differences between adjacent pixels. The optimum number of samples per row can be found be varying the number of samples per row, constructing each image, and evaluating its smoothness.

Another, more computationally efficient method for determining the number of samples per row uses autocorrelation. Figure 8 shows a zoomed view of the autocorrelation of two different signals. Autocorrelation is a measure of how similar a signal is to itself at different lags. At lags that are a multiple of the number of samples per row, the autocorrelation will have a local maxima. This phenomenon can be seen in Figure 8b and Figure 8d. In both examples, the number of samples per row is about 500. This causes

local maxima at lags of about 500, 1000, 1500, and 2000. The heights of the local maxima decrease as the lag increases. The lag of the first local maximum is the number of samples per row. The local maxima occur because SEM images are natural images. Natural images have low spatial frequencies. In other words, pixels near each other are likely to have the same value. The pixels of two adjacent rows will have nearly the same values. At lags that are multiples of the number of samples per row, the sample values are highly correlated. This is indicated by large peaks in the autocorrelation.

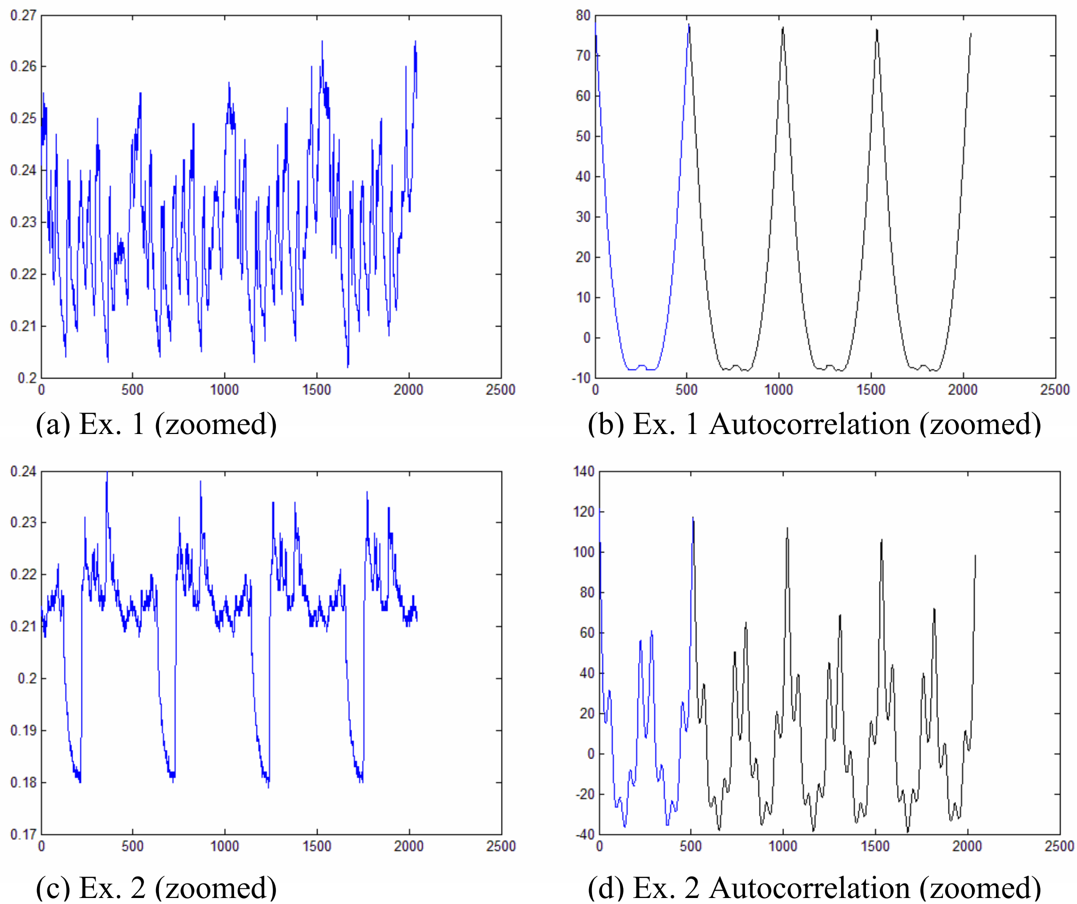

(a) Ex. 1 (zoomed) (b) Ex. 1 Autocorrelation (zoomed)

(c) Ex. 2 (zoomed) (d) Ex. 2 Autocorrelation (zoomed)

Figure 8: (a) The first 2000 samples from example 1 and (b) the autocorrelation for example 1. (c) The first 2000 samples from example 2 and (d) the autocorrelation of example 2.

5.6 Number of Rows (N_r)

The number of rows sets the height of the final image. The number of rows is not a critical parameter to determine. Reducing the number of rows will crop rows from the bottom of the image.

The number of rows is an attribute of the raster pattern. The number of rows can be approximated by estimating the number of lines on the SEM cathode ray tube. For an SEM, this value is usually approximately a power of 2, such as 256, 512, or 1024. In general, this value can be any natural integer.

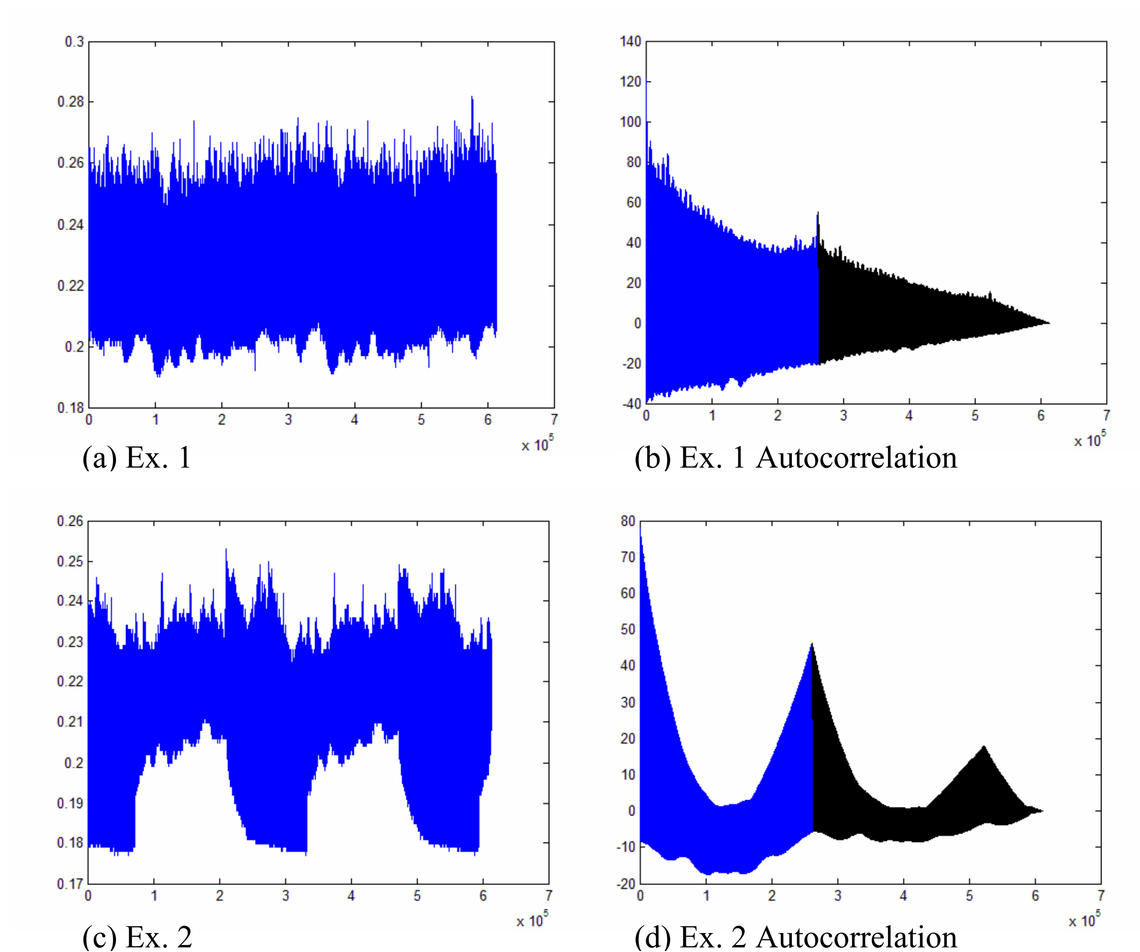

Figure 9: (a) All of the samples from example 1 and (b) the autocorrelation for example 1. (c) All of the samples from example 2 and (d) the autocorrelation of example 2.

The number of rows can also be inferred from the series of samples. A computationally efficient method for determining the number of rows uses autocorrelation. Figure 9 shows the autocorrelation of two different signals. At lags that are a multiple of the total number of samples in the image, the envelope of the autocorrelation will have local maxima. This phenomenon can be seen in Figure 9b and Figure 9d. In both examples, the total number of samples in the image is about is about 260,000. This causes local maxima at lags of about 260,000 and 520,000. The heights of the local maxima decrease as the lag increases. The lag of the first local maxima is the total number of samples in the image. The local maxima of the envelope occur when complete raster scan align with each other. In each of the examples in Figure 9, there are about 2.3 raster scans. This method assumes that there is at least 2 raster scans so that there is at least 1 complete, continuous raster scan in the series of samples. The total number of samples in the image is the product of the number of samples per row and the number of rows.

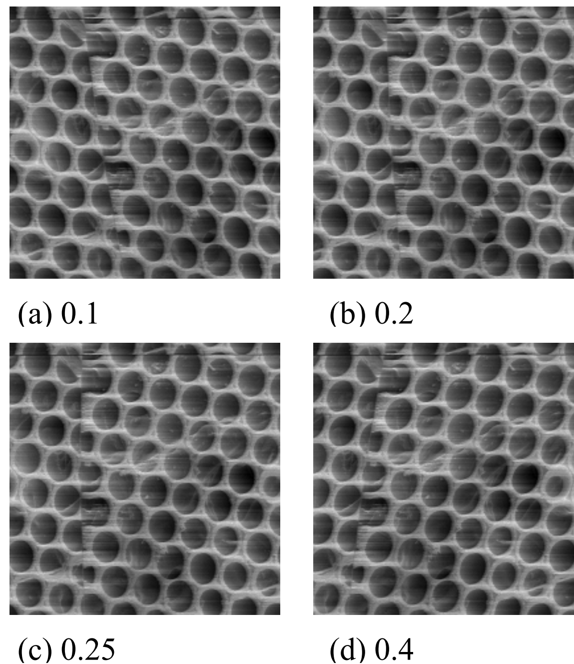

Figure 10: Varying Number of Samples between Rows (N_{sbr})
$N_r = 512$, $N_{spr} = 511$, $N_{is} = 0$

5.7 Number of Samples between Rows (N_{sbr})

The number of samples between rows affects the skew of the final image. Decreasing the number of samples between rows will skew the image to the left. Increasing the number of sample between rows will skew the image to the right. This can be seen by the change in the slope of the slanted line. Figure 10 shows how varying the number of samples per row affects the image. The image with the optimum number of samples between rows is in Figure 10c.

If the number of samples per row is optimized, then the number of samples between rows can be visually optimized. When the number of samples per row is optimized, the image will appear to be skewed and will contain a slanted and a horizontal line. As shown in Equation 2, the slope of the slanted line is the number of samples between rows.

$$N_{sbr} = M_{slanted} \tag{2}$$

In Equation 2, N_{sbr} is the number of samples between rows, and $M_{slanted}$ is the slope of the slanted line. A user interface can be created so that the user can select two points on the slanted line.

A computer vision approach can be applied to automatically detect the slanted line and calculate the slope. The edge detection algorithm must be able to distinguish the slanted line from other lines in the image.

5.8 Number of Initial Samples (N_{is})

The number of initial samples removes pixels from the beginning of the set of samples. Figure 11 shows how varying the number of initial samples affects the final image. As the number of initial samples increases, the horizontal line moves up and the vertical line moves to the left. The image with the optimum number of initial samples is in Figure 11c. This is the fully optimized, final image.

If the number of samples between rows is optimized, then the number of initial samples can be visually optimized. When the number of samples per row and the number of samples between rows are both optimized, the image will not be skewed and will contain a vertical and a horizontal line. The vertical and horizontal lines are the right/left and top/bottom edges of the image, respectively. As shown in Equation 3, the number of

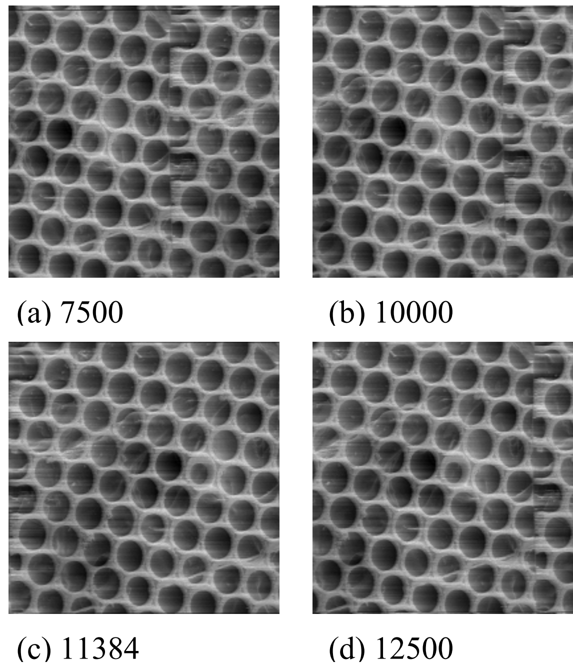

Figure 11: Varying Number of Initial Samples (N_{is})
$N_r = 512$, $N_{spr} = 511$, $N_{sbr} = 0.25$

initial samples is related to the horizontal and vertical lines.

$$N_{is} = Y_h \cdot N_{spr} + X_v \tag{3}$$

In Equation 3, N_{is} is the number of initial samples, N_{spr} is the number of samples per row, Y_h is the y-intercept of the horizontal line, and X_v is x-intercept of the vertical line. A conventional coordinate system for Y_h and X_v is used such that the origin is the top left corner of the image, the y-axis increases going down the image, and the x-axis increases going right on the image. A user interface can be created so that the user can select a point on the vertical line and a point on the horizontal line.

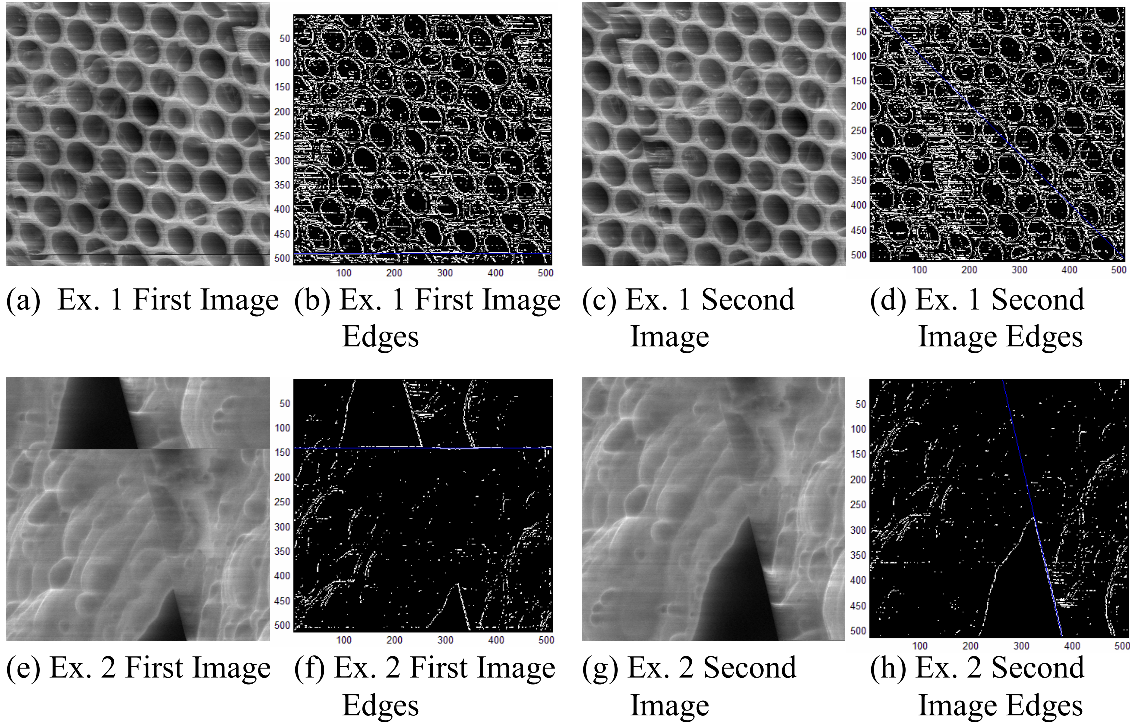

(a) Ex. 1 First Image (b) Ex. 1 First Image Edges (c) Ex. 1 Second Image (d) Ex. 1 Second Image Edges

(e) Ex. 2 First Image (f) Ex. 2 First Image Edges (g) Ex. 2 Second Image (h) Ex. 2 Second Image Edges

Figure 12: Example 1 (a) First image (b) Edges of first image (c) Second image (d) Edges of second image and Example 2 (e) First image (f) Edges of first image (g) Second image (h) Edges of second image

A computer vision approach can be applied to automatically detect the vertical and horizontal lines and then calculate their intercepts. The edge detection algorithm must be able to distinguish the true vertical and horizontal lines.

Figure 12 illustrates that the horizontal and slanted lines can be detected using an edge detection algorithm from computer vision. The first images, shown in Figure 12a and Figure 12e, are constructed using the optimum values for the number of samples per row and the number of rows. The number of initial samples and the number of samples between rows are both assumed to be zero. Figure 12b and Figure 12f show the edges of the first image. The horizontal line is easily detected by summing the number of edges in each row. The number of pixels above the horizontal line is a first estimate for the number of initial samples. Using this estimate, the second images, shown in Figure 12c and Figure 12g, are constructed. The second images will only contain a slanted line. Figure 12d and Figure 12h show the edges of the second image. A Hough transform can be used to find the most prominent slanted line in the image. This approach is successful for some but not all images. This approach found the correct line in Figure 12h, but the incorrect line in Figure 12d. A better approach for detecting the slanted line is essential for a fully autonomous system. However, the image can be corrected with user input. The corrected, final images are in Figure 13a and Figure 13b.

6. Results

A LabVIEW user interface was developed to acquire a set of samples, perform the algorithm with user input, and then save the resulting image. The LabVIEW interface acquires samples from the Data Translations DT9832. An improved Matlab user interface

was also developed. The Matlab user interface can perform the algorithm with user selected levels of autonomy, and save the resulting image.

Several sets of samples were obtained from an analog SEM. The SEM was set to a scan rate of about 60 scan lines per second. There are about 512 scan lines on the SEM. In order to achieve a correctly proportioned, square image, there must be about 512 samples per row. The Data Translation DT9832, an analog to digital converter, was set to a sampling rate of 30659 samples per second. Other data sets were collected at various other sampling rates. Figure 13a and 13b contains two images that were acquired using the algorithm. Figure 13c and 13d contains the same images obtained using a SEM digital image capture system that actively controls electron beam position. The image capture system automatically performs digital image processing on the acquired image.

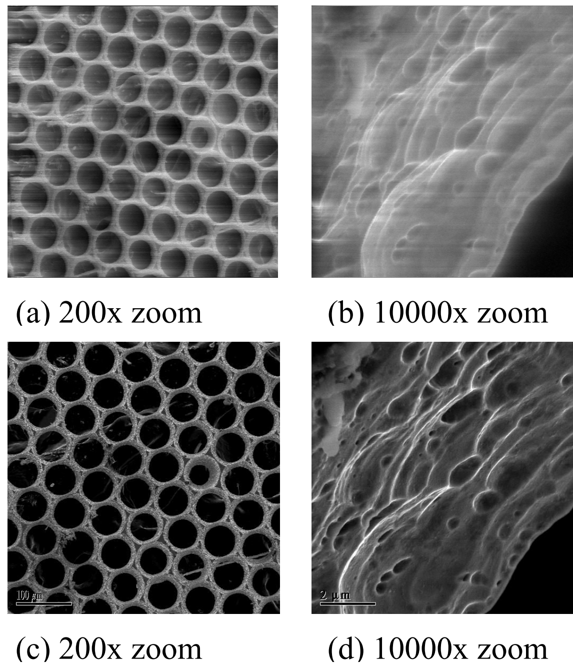

Figure 13: (a) (b) SEM images acquired using algorithm compared to (c) (d) SEM images acquired using an SEM digital image capture system.

7. Limitations

The proposed method has some limitations. In some situations, the model parameters are difficult to determine. The number of samples between rows (N_{sbr}) and the number of initial samples (N_{is}) control the positions of the left/right edge of the image and the top/bottom edge of the image. The parameters are determined by detecting the left/right edge of the image, which is the slanted or vertical line, and the top/bottom edge of the image, which is the horizontal line. Figure 14 demonstrates some limitations of the methods by showing some example cases. Figure 14a shows a case where there is a strong vertical and a strong horizontal edge. In this case, the edges can be easily be detected and the true image, shown in Figure 14e, can be formed. Figure 14b shows a

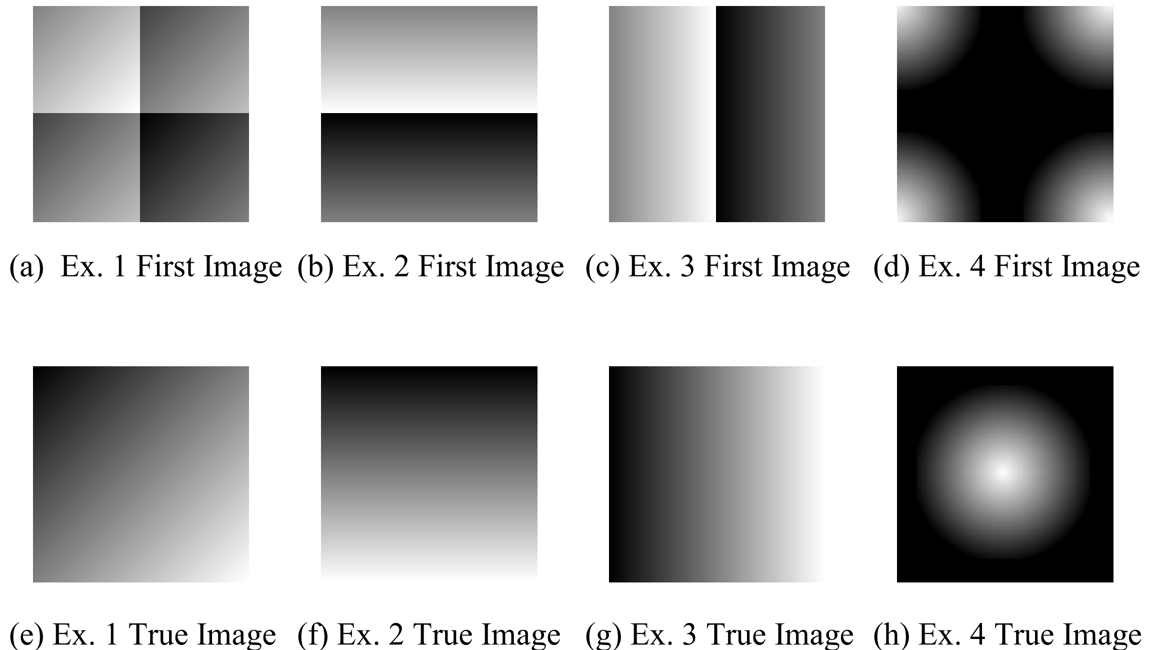

Figure 14: (a) Example of a first image with horizontal and vertical edges. (b) Example of a first image with only a horizontal edge. (c) Example of a first image with only a vertical edge. (d) Example of a first image with no edges. (e) (f) (g) (h) Corresponding true image that should, but in some cases would not, be formed.

case where there is only a strong horizontal edge. In this case, the horizontal edge can be easily be detected and the true image, shown in Figure 14f, can be formed. However, if there were other objects within the gradient, then they could be shifted to the left or right. Figure 14c shows a case where there is only a strong vertical edge. In this case, the vertical edge can be easily be detected and the true image, shown in Figure 14g, can be formed. However, if there were other objects within the gradient, then they could be shifted to the up or down. Figure 14d shows a case where there are no strong edges. In this case, the edges of the image cannot be detected and the true image, shown in Figure 14h, would not be formed. To summarize, from Figure 14, it is shown that the true image is formed when both the horizontal and vertical edges are both detected. This limitation must be acceptable if this method is used for digital image acquisition.

8. Discussion

The proposed method can easily connect to most SEMs. All SEMs have a secondary electron detector in the SEM column. On most SEMs the wires connecting the electron detector to the SEM control panel are accessible. These wires can be tapped into at the connection to the SEM control panel. With the other methods proposed in related work, complex circuits must be manufactured or sync signals must be located within the SEM control panel.

The proposed method is passive. The normal functionality of the SEM is not changed by digital image acquisition system. The method does not have to control the position of the

electron beam. Since the proposed system does not control the electron beam, it requires less electronic hardware in its implementation.

In the proposed method, a digital image is formed by sampling the electron detector with an analog to digital converter. Unlike previous approaches, the proposed method is not synchronized with the electron beam position. The proposed method infers the electron beam position from the samples collected from the electron detector. The method uses less sensory data than previous approaches. Therefore, the method can be implemented as a redundant system for previous approaches.

As seen in the related work, several solutions have been proposed for acquiring digital images from SEMs. The proposed solution requires the least amount of hardware. It only requires a single analog to digital converter connected to a personal computer. By reducing the hardware complexity, the software complexity increases significantly. However, the proposed algorithm is feasible due to the increased computational power of personal computers.

As stated previously, the proposed method has some limitations. In some images, the optimization parameters are difficult to determine. The top and bottom of the image must form an edge that can be detected. Likewise, a right and left parts of the image must form an edge that can be detected. This limitation is acceptable since these edges are usually detectable.

As seen in the images in Figure 7, the optimization of the number of samples per row is very important. If the number of samples per row varies too far from the optimum value, then the image becomes too skewed. The skew inhibits visual optimization of the other parameters.

9. Future Work

In future work, the method can be further improved through a better line detection algorithm. The slanted line, that represents the left and right edges, is difficult to detect. The line detection could be improved by only detecting straight edges instead of all edges. Texture can also be used to improve the line detection algorithm.

Also, in the proposed method, the user must select a sampling rate for the analog to digital converter such that the final image is not stretched horizontally. The final image must have a specific number of samples per row so that the image will have the same horizontal and vertical resolution. In further work, the sampling rate of the analog to digital converter can be automatically varied to obtain a user-specified number of samples per row.

Finally, some image processing techniques can be used to increase the contrast, sharpness, and quality of the acquired images. Other SEM image acquisition systems use digital image processing to enhance the image quality.

10. Further Applications

The method described in this thesis can be applied to other applications. The model may need to be altered for the specific application. The general guidelines for applying the method are as follows. First, develop a model for relating the collected data to the desired results. The model should incorporate a smoothness constraint, which promotes the clustering of similar data. Next, correlate the data to determine which elements are most similar. The correlation assists in finding similar data. The model is used to interpret the correlation. Finally, the collected data can be processed to best fit the model.

The method can be modified for digital image acquisition from video signals. The model would be similar to the model proposed in this thesis. However, the model is dependent on the video signal being digitized. For example, color video contains multiple components for each pixel in the final image. The components are encoded differently depending on the video transmission protocol. Regardless of the transmission protocol, each of the components of final color image will be smooth. Therefore, a smoothness constraint can be applied to each of the components in the final color image.

The method can be applied to the simultaneous localization and mapping (SLAM) problem in the field of mobile robotics. In the SLAM problem, the mobile robot is developing a map of the environment, while at the same time, localizing itself in the environment. The mobile robot must estimate its position based on observations from its sensors. Similarly, in this thesis, the position of the electron beam must be estimated using data from an electron detector sensor. However, the SLAM model would be

significantly different than the model proposed in this paper. It must incorporate other knowledge related to the SLAM problem. The SLAM model may incorporate information about the reaction of the robot to different sensory data. It could incorporate a smoothness constraint, which relates similar sensory observations to the same location in the environment.

The method can be modified to generate a topographical map of a surface that has been scanned by a light detection and ranging (LIDAR) system. In this problem, a topographical map is generated from a set of one dimensional scans of the surface. The model would incorporate information about how the LIDAR system is scanned over the surface. The final topographical map should be smooth. Therefore a smoothness constraint can be applied to the final topographical map.

11. Conclusion

This thesis presented a novel method for obtaining digital images from an SEM. The minimal hardware requirements for the method were presented. Both autonomous and user assisted variations of the method were described. The method is unique because the digital image was formed by sampling the electron detector without knowledge of the location of the electron beam. The method was used to acquire some SEM images. They were compared to SEM images acquired using a commercial SEM digital image capture system. Future work can improve the quality of the acquired images and increase the autonomy of the algorithm.

REFERENCES

[1] J. I. Goldstein, D. E. Newbury, P. Echlin, D. C. Joy, C. Fiori, and E. Lifshin, *Scanning Electron Microscopy and X-Ray Microanalysis*, New York, NY: Plenum, 1984.

[2] J. A. Eichmeier and M. Thumm, *Vacuum Electronics: Components and Devices*, Springer, 2008.

[3] V. E. Cosslett, *Introduction to Electron Optics: the production, propagation, and focusing of electron beams*, Clarendon Press, 1946.

[4] O. C. Wells and D. C. Joy, "The early history and future of the SEM," *Surface and Interface Analysis*, vol. 38, pp. 1738-1742, 2006.

[5] M. Meyyappan, *Carbon Nanotubes: Science and Applications*, CRC Press, 2004.

[6] B. P. Ribaya, J. Leung, P. Brown, M. Rahman and C. V. Nguyen, "A study on the mechanical and electrical reliability of individual carbon nanotube field emission cathodes," *Nanotechnology*, vol. 19, 185201, 2008.

[7] J. L. Killian, N. B. Zuckerman, D. L. Niemann, B. P. Ribaya, M. Rahman, R. Espinosa, M. Meyyappan and C. V. Nguyen, "Field emission properties of carbon nanotube pillar arrays," *J. Applied Physics*, vol. 103, 064312, 2008.

[8] D. L. Niemann, J. Silan, J. L. Killian, K. R. Schwanfelder, M. Rahman, M. Meyyappan, and C. V. Nguyen, "Carbon Nanotube Field Emission Devices with Integrated Gate for High Current Applications," *IEEE Conference on Nanotechnology*, pp. 456-459, 2008.

[9] D. L. Niemann, J. Silan, J. L. Killian, B. Ribaya, M. Rahman, C. V. Nguyen, "Gated carbon nanotube pillar arrays for high current applications," *IEEE IVEC*, pp.437-438, 2008.

[10] B. P. Ribaya, D. L. Niemann, J. Makarewicz, N. G. Gunther, C. V. Nguyen, M. Rahman, "Dynamic Properties of Individual Carbon Nanotube Emitters for Maskless Lithography," *IEEE IVEC*, pp. 439-440, 2008.

[11] B. Ribaya, D. Niemann, N. Gunther, M. Rahman, C. V. Nguyen, "An Experimental Study and Modeling of the Field Emission Properties of an Isolated Individual Multi-Walled Carbon Nanotube," *IEEE IVEC*, pp. 505-506, 2006.

[12] B. P. Ribaya, D. L. Niemann, J. Makarewicz, N. G. Gunther, C. V. Nguyen and M. Rahman, "An empirical study of dynamic properties of an individual carbon nanotube electron source system," *ISDRS*, 2007.

[13] B. P. Ribaya, D. L. Niemann, J. Makarewicz, N. G. Gunther, C. V. Nguyen and M. Rahman, "An empirical study of dynamic properties of an individual carbon nanotube electron source system," *Solid State Electronics*, vol. 52, pp. 1680-1686, 2008.

[14] B. P. Ribaya, *Fabrication of Isolated Individual Multi-walled Carbon Nanotube Field Emission Cathodes*, Santa Clara, Santa Clara University School of Engineering, 2006.

[15] D. L. Niemann, *Experimental and theoretical investigations of field emission in carbon nanotubes and their multiscale integrated systems*, Santa Clara, Santa Clara University School of Engineering, 2008.

[16] D. L. Niemann, B. P. Ribaya N. Gunther, M. Rahman, J. Leung and C. V. Nguyen, "Effects of cathode structure on the field emission properties of individual multi-walled carbon nanotube emitters," *Nanotechnology*, vol. 18, 485702, 2007.

[17] O. H. Kapp, D. R. Smith, G. Jendraszkiewicz, I. Gorodezky, K. Kim, and A.V. Crewe, "A flexible instrument control and image acquisition system for a scanning electron microscope," *J. Micros.*, vol. 223, pp. 140-149, 2006.

[18] S. Ruan, and O. H. Kapp, "An image acquisition system built with a modular frame grabber for scanning electron microscopes," *Rev. Sci. Instrum.*, vol. 66, pp. 4539-4543, 1995.

[19] M. T. Postek, and A.E. Vlad´ar, "Digital imaging for scanning electron microscopy," *Scanning*, vol. 18, pp. 1–7, 1996.

[20] W. M. Ang, T. McMahon, D. Schulte, and L. Ungier, "Inexpensive digital image acquisition for scanning electron microscopes," *Rev. Sci. Instrum.*, vol. 66, pp. 1151-1153, 1995.

[21] S. Russev, G. Tsutsumanova, S. Angelov, and K. Bachev, "An electron beam lithography and digital image acquisition system for scanning electron microscopes," *J. Micros.*, vol. 226, pp. 64-70, 2006.

[22] A. Gebert, and G. Preiss, "A simple method for the acquisition of high quality digital images from analog scanning electron microscopes," *J. Micros.*, vol. 191, pp. 297-301, 1998.

[23] R.F. Egerton, and L. Wan, "Low-cost image-capture system for a scanning electron microscope," *J. Micros.*, vol. 191, pp. 113-115, 1998.

[24] M. A. Dubson, and Q. Zhu, “Digital images from your old scanning electron microscope,” *Rev. Sci. Instrum.*, vol. 63, pp. 4461-4462, 1992.